Magnetoplasmonic Dipole Nanoantenna for Reconfigurable Optical Communications

Gabriel H. B. Damasceno , William O. F. Carvalho , Arismar Cerqueira S. Jr. , and J. R. Mejía-Salazar

***Abstract*— We numerically show that magneto-optical (MO) effects in magnetoplasmonic dipole nanoantennas, built by plasmonic ferromagnetic materials, enable active beam steering of the radiated fields. Our design, working at the visible wavelength $\lambda = 690$ nm, is promising for applications in intra- and inter-chip reconfigurable optical nanolinks for future 6G communication networks.**

***Keywords*— 6G, Beam steering, Dipole, Magnetoplasmonic, Nanoantennas.**

I. Introduction

The future deployment of 6G technologies will require ultra high transmission rates and very low end-to-end latency [1], to avoid information bottlenecks, where the transmitters and receivers must process thousands of terabits per second (Tbps). Therefore, faster and more robust on-chip devices will be required for successful massive data processing. A promising approach to support the elevated speed rate and, simultaneously, provide higher on-chip integrability is the use of plasmonic technologies [2]. In contrast to conventional photonic-nanoelectronic approaches, where minimum sizes are limited by diffraction laws and interconnection delays, plasmonic fields provides remarkably data rates and extreme miniaturization for on-chip optical communications.

Plasmonics refers to the technological exploitation of the resonant coupling of electromagnetic waves to collective free-electron oscillations on metallic surfaces. In particular, plasmonic nanoantennas for optical wireless broadcasting at chip-scale are deserving attention to surpass optical absorption from waveguides, providing new paths for future nanoscale wireless interconnections [3]. The physical principle behind plasmonic nanoantennas lies in radiating localized surface plasmon resonances (LSPRs) supported by finite nanometer-scale metallic structures. Significantly, these nanostructures can be designed analogously to conventional radio frequency (RF) antennas, but tailored to operate at optical frequencies.

Gabriel H. B. Damasceno, NanoPhotonics Group and WOCA Labs, Inatel, Santa Rita do Sapucaí-MG, e-mail: gdamasceno@get.inatel.br; William O. F. Carvalho, NanoPhotonics Group, Inatel, Santa Rita do Sapucaí-MG, e-mail: william.carvalho@dtel.inatel.br. A. Cerqueira Sodré Jr., WOCA Labs, Inatel, Santa Rita do Sapucaí-MG, e-mail: arismar@inatel.br; J. R. Mejía-Salazar, NanoPhotonics Group, Inatel, Santa Rita do Sapucaí-MG, e-mail: jrmejia@inatel.br. Partial financial support was received from RNP, with resources from MCTIC, Grant No. 01245.010604/2020-14, under the Brazil 6G project of the Radiocommunication Reference Center (Centro de Referência em Radiocomunicações - CRR) of the National Institute of Telecommunications (Instituto Nacional de Telecomunicações - Inatel), Brazil. We also acknowledge the financial support from the Brazilian agencies Coordenação de Aperfeiçoamento de Pessoal de Nível Superior - Brasil (CAPES) - Finance Code 001, the National Council for Scientific and Technological Development-CNPq (314671/2021-8) and FAPESP (2021/06946-0).

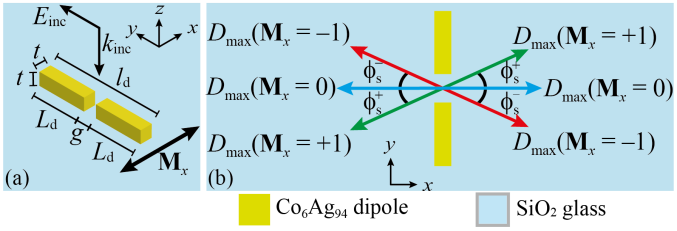

Fig. 1: Schematic of the magnetoplasmonic dipole nanoantenna.

Indeed, this approach has been successfully applied in various context, including communications, medicine, quantum sources, sensing, photovoltaics, optical computing, spectroscopy, and many others [4].

Although magneto-optical (MO) effects are receiving attention for new active nanophotonic devices [5], there is a lack of application in optical nanoantennas for wireless communications. In this paper, we numerically demonstrate (for the first time) that the radiated field from a half-wave dipole nanoantenna can be actively manipulated using applied magnetic fields. We hope that results from this work stir significant interest to develop new mechanism for beam steering in future nanoscale optical communications.

II. Design and Modeling

Figure 1(a) schematically shows the magnetoplasmonic dipole nanoantenna. The device is built by ferromagnetic cobalt-silver alloy (Co_6Ag_{94}), embedded in silica (SiO_2). We use a s-polarized wave (in our case, $E_{inc} = E_y e^{-ik_{inc}z}$) impinging on the nanoantenna, properly designed to exhibit the desired LSPR. Each dipole arm has a length L_d, width t and height t, and a gap g between the arms, totalizing a dipole length l_d. As indicated in Figure 1(b), the scattered wave can be steered according to the magnetization direction on the structure, as illustrated with the red, blue and green arrows.

In contrast to the RF domain, where a half-wave dipole antenna has a length of $\lambda/2$, metallic nano-components cannot be considered perfect conductors at the optical regime [2]. In fact, the resonance wavelength of a dipole nanoantenna is strongly dependent on the material building permittivity and geometrical designs. An useful parameter to guide the design of optical dipole nanoantennas is the effective wavelength, defined as $\lambda_{eff} = a + b(\lambda/\lambda_p)$ [6], where a and b are factors determined by the metallic properties and the surrounding media, λ is the incident wavelength and λ_p is the plasma wavelength. Moreover, due to the intrinsic MO activity of the Co_6Ag_{94} building material, the anisotropic permittivity tensor

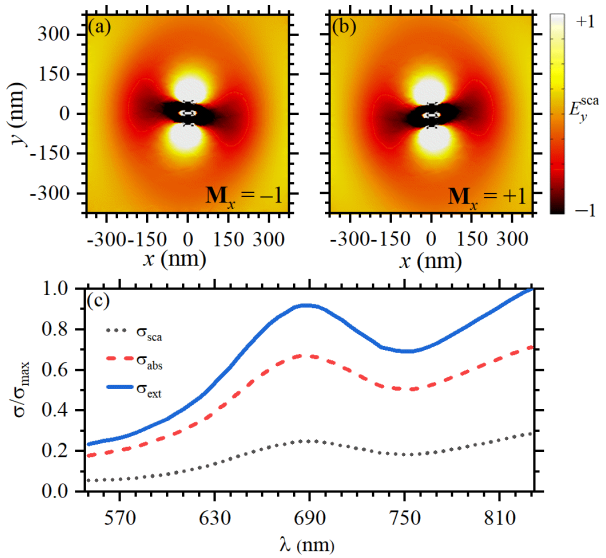

Fig. 2: Near-fields for (a) $\mathbf{M}_x = -1$ and (b) $\mathbf{M}_x = +1$, whilst in (c) is observed the cross-sections efficiencies along the wavelength.

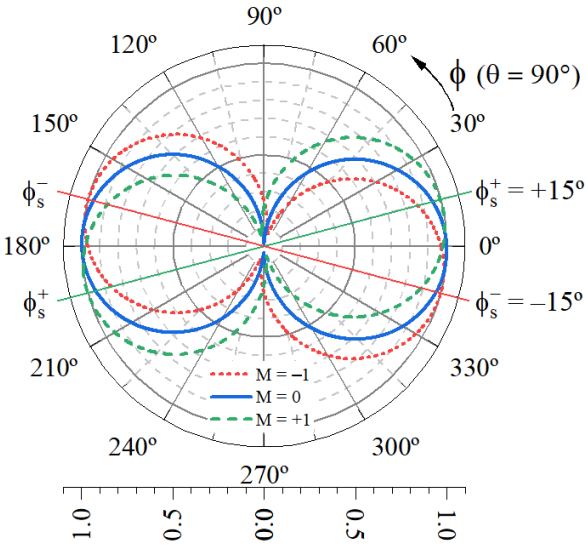

Fig. 3: Azimuthal 2D normalized far-field for $\mathbf{M}_x = 0$ (black solid), $\mathbf{M}_x = -1$ (red dotted) and $\mathbf{M}_x = +1$ (blue dashed) curves. A far-field steering of $\pm 15°$ ($\mathbf{M}_x = \pm 1$) is observed.

of the nanoantenna is represented by [7]:

$$\tilde{\varepsilon}_{\mathrm{Co_6Ag_{94}}} = \begin{pmatrix} \varepsilon_{\mathrm{Co_6Ag_{94}}} & 0 & 0 \\ 0 & \varepsilon_{\mathrm{Co_6Ag_{94}}} & i\varepsilon_{yz}\mathbf{M}_x \\ 0 & -i\varepsilon_{zy}\mathbf{M}_x & \varepsilon_{\mathrm{Co_6Ag_{94}}} \end{pmatrix}, \quad (1)$$

where the diagonal components are isotropic, whereas the off-diagonal values depend on the magnetization amplitude and direction along the x-axis. Remarkably, the beam steering is only allowed for $\mathbf{M}_x = \pm 1$, in relation to Figure 1. The permittivity values (for $\lambda = 690$ nm) used in the simulations are $\varepsilon_{\mathrm{Co_6Ag_{94}}} = -12.083 + i1.766$, $\varepsilon_{yz} = \varepsilon_{zy} = -3.126 - i2.032$ [8] and $\varepsilon_{\mathrm{SiO_2}} = 2.163$ [9].

The numerical results were obtained using finite element method (FEM) simulations with the commercial software COMSOL Multiphysics®. An optimized mesh-size was also used for accurateness in the numerical results. Finally, to avoid numerical reflections at the edge of the structure, we used perfectly matched layers (PMLs) on all boundaries.

III. Results and Discussion

The geometry of the structure was numerically optimized to work at $\lambda = 690$ nm, i.e., where the maximum extinction (σ_{ext}) cross-section (the sum of the scattering (σ_{sca}) plus the absorption (σ_{abs}) cross-sections) is achieved. The optimization was carried out through a numerical swept of l_{d} for the half-wave dipole, finding $l_{\mathrm{d}} = 84$ nm, $L_{\mathrm{d}} = 37$ nm, $g = 10$ nm and $t = 30$ nm for this case.

Figures 2(a)-(b) show the near-fields of the normalized scattered electric field E_y^{sca}, for $\mathbf{M}_x = -1$ and $\mathbf{M}_x = +1$, respectively. Calculations were made for $\lambda = 690$ nm, where the maximum for σ_{ext}, σ_{sca}, and σ_{abs} is found, as seen from Figure 2(c). Although a detrimental behavior $\sigma_{\mathrm{abs}} > \sigma_{\mathrm{sca}}$ is observed, due to the optical losses from the $\mathrm{Co_6Ag_{94}}$ material, the high-level of optical beam steering noticed from Figure 3 indicates a new way for active wireless optical communications at the chip-scale level. This last figure comparatively shows the 2D normalized azimuthal radiation patterns for $\mathbf{M}_x = 0$ (black solid), $\mathbf{M}_x = -1$ (red dotted) and $\mathbf{M}_x = +1$ (blue dashed).

IV. Conclusions and Outlook

Summarizing, we demonstrated a new concept for active beam steering from magnetoplasmonic dipole nanoantennas. The simultaneous ferromagnetic and metallic properties of $\mathrm{Co_6Ag_{94}}$ were used for active manipulation of the radiated field. Our idea has potential applications in the design and development of reconfigurable inter-/intra chip wireless nanolinks for future 6G integrated optical networks devices.

References

[1] S. Dang, O. Amin, B. Shihada, and M.-S. Alouini, "What should 6G be?" *Nat. Electron.*, vol. 3, pp. 20–29, 2020.

[2] W. O. F. Carvalho and J. R. Mejía-Salazar, "Plasmonics for telecommunications applications," *Sensors*, vol. 20, no. 9, p. 2488, 2020.

[3] S. Lechago, C. García-Meca, A. Griol, M. Kovylina, L. Bellieres, and J. Martí, "All-silicon on-chip optical nanoantennas as efficient interfaces for plasmonic devices," *ACS Photonics*, vol. 6, no. 5, pp. 1094–1099, 2019.

[4] A. E. Krasnok, I. S. Maksymov, A. I. Denisyuk, P. A. Belov, A. E. Miroshnichenko, C. R. Simovski, and Y. S. Kivshar, "Optical nanoantennas," *Phys.-Uspekhi*, vol. 56, no. 6, pp. 539–564, jun 2013.

[5] I. S. Maksymov, "Magneto-plasmonic nanoantennas: basics and applications," *Rev. Phys.*, vol. 1, pp. 36–51, 2016.

[6] L. Novotny, "Effective wavelength scaling for optical antennas," *Phys. Rev. Lett.*, vol. 98, no. 26, p. 266802, 2007.

[7] M. G. Barsukova, A. S. Shorokhov, A. I. Musorin, D. N. Neshev, Y. S. Kivshar, and A. A. Fedyanin, "Magneto-optical response enhanced by mie resonances in nanoantennas," *ACS Photonics*, vol. 4, no. 10, pp. 2390–2395, 2017.

[8] S.-Y. Wang, W.-M. Zheng, D.-L. Qian, R.-J. Zhang, Y.-X. Zheng, S.-M. Zhou, Y.-M. Yang, B.-Y. Li, and L.-Y. Chen, "Study of the Kerr effect of $\mathrm{Co}_x\ \mathrm{Ag}_{100-x}$ granular films," *J. Appl. Phys.*, vol. 85, no. 8, pp. 5121–5123, 1999.

[9] L. Gao, F. Lemarchand, and M. Lequime, "Refractive index determination of $\mathrm{SiO_2}$ layer in the UV/Vis/NIR range: Spectrophotometric reverse engineering on single and bi-layer designs," *J. Eur. Opt. Society-Rapid Publ.*, vol. 8, 2013.